# ANALYSIS OF NEAR RECTILINEAR HALO ORBIT INSERTION WITH A 40-KW SOLAR ELECTRIC PROPULSION SYSTEM

**Steven L. McCarty[*], Waldy K. Sjauw[†], Laura M. Burke[‡], Melissa L. McGuire[§]**

This paper examines two low thrust insertion options for delivery of a 40-kW solar electric propulsion spacecraft to a Near Rectilinear Halo Orbit (NRHO). One option considered is a trans-lunar injection launch as a co-manifested payload on the Space Launch System. For this option, a reference trajectory is designed and a scan of launch dates is completed to understand the propellant mass sensitivity. A 15-day period cyclical variation in required propellant is observed that is attributed to solar gravity effects. A second option considered is to launch on a smaller commercial launch vehicle to a less energetic elliptical orbit and use SEP to spiral out to NRHO. For this option, analysis is completed to understand the trades between delivered mass to NRHO, total propellant required, time of flight, and solar array degradation. Results show that, while launching to lower altitudes can deliver greater payload mass to NRHO, significant solar array degradation can occur. In addition to a generic dataset that can be applied to any launch vehicle, spiral trajectory results are presented specific to launch on an Atlas V 551 and Falcon 9.

## INTRODUCTION

Near Rectilinear Halo Orbits (NRHOs) have been shown to be of particular interest as staging orbits for human exploration of the Moon[1–3] and were previously the crew rendezvous orbit for the cancelled Asteroid Redirect Mission.[4] A high power solar electric propulsion (SEP) spacecraft has been studied as a building block for a larger crewed station in NRHO that could provide power, station keeping, attitude control, and primary propulsion for transfer between cislunar orbits.[5] This paper examines two options for low thrust insertion of a 40-kW SEP spacecraft and potential additional payload to a desired NRHO.

One option considered is to launch as a co-manifested payload on the Space Launch System (SLS). A reference trajectory has been designed that targets an outbound Lunar Gravity Assist (LGA) before eventual insertion of an assumed spacecraft into the NRHO. From this reference trajectory, analysis has been completed to understand how the propellant required to complete the insertion varies with launch date. In general, the results are considered applicable to other launch

[*]Mission Design Engineer, Mission Architecture and Analysis Branch, NASA Glenn Research Center, 21000 Brookpark Road, Cleveland, OH, 44135

[†]Aerospace Engineer, Mission Architecture and Analysis Branch, NASA Glenn Research Center, 21000 Brookpark Road, Cleveland, OH, 44135

[‡]Aerospace Engineer, Mission Architecture and Analysis Branch, NASA Glenn Research Center, 21000 Brookpark Road, Cleveland, OH, 44135

[§]Branch Chief, Mission Architecture and Analysis Branch, NASA Glenn Research Center, 21000 Brookpark Road, Cleveland, OH, 44135

vehicles that can deliver adequate mass to trans-lunar injection (TLI), though the reference trajectory does include some SLS specific constraints.

A second option considered is to launch on a smaller commercial launch vehicle to a less energetic elliptical orbit and use SEP to spiral out to NRHO. This insertion type may be attractive if the chosen launch vehicle cannot deliver enough mass to TLI. For this option, analysis has been completed to understand the trades between mass inserted to NRHO, total propellant required, time of flight (TOF), and solar array performance for launch on Falcon 9 and Atlas V 551.

Though not considered here, ballistic lunar transfers may also be used to insert into the NRHO.[6] Such trajectories require launch energies similar to the SLS option, but are not feasible in this case primarily because of a 100-day TOF constraint imposed on this insertion option.

## ANALYSIS ASSUMPTIONS

This section outlines the assumptions used throughout the analysis, unless otherwise noted, including those for the spacecraft performance and the target NRHO.

### Spacecraft

The spacecraft is assumed to carry a high-power SEP system consisting of three 13.3 kW thrusters operating at a maximum of 40 kW (rounded from 39.9) at 1 au from the Sun. Available power is assumed to decrease as $1/R^2$ when operating at distances greater than 1 au. In addition, no constraints are placed on the thrust direction. A duty cycle of 90% is used for all thrust arcs to provide margin for thrust outages and other non-thrusting activities, which is modeled as a proportionate decrease in thrust and mass flow rate. Unless otherwise noted, the spacecraft wet mass is assumed to be 6,500 kg (this is also the assumed maximum SLS co-manifested payload mass capability). A summary of these and other spacecraft assumptions are shown in Table 1.

The assumed performance for a single thruster as a function of input power is shown in Table 2. Available power is evenly distributed between all operating thrusters, with each operating at a minimum and maximum power of 7 kW and 13.3 kW, respectively.

**Table 1. Summary of the spacecraft ground rules and assumptions**

| Parameter | Value | Note |
|---|---|---|
| Wet Mass | 6,500 kg | Also the assumed maximum SLS co-manifested payload mass capability |
| Power | 40 kW | Maximum at 1 au |
| Number of Thrusters | 3 | - |
| Power Model | $1/R^2$ | No increase in power for R less than 1 au |
| Duty Cycle | 90% | For thrust outages and non-thrusting activities |
| Checkout Period | 14 days | Minimum time to checkout spacecraft before SEP thrusting |
| RCS $I_{sp}$ | 230 s | Specific impulse for impulsive burns, if necessary |

**Table 2. SEP thruster performance as a function of input power**

| Power (kW) | Thrust (mN) | $\dot{m}$ (mg/s) | $I_{sp}$ (s) |
|---|---|---|---|
| 13.3 | 566.3 | 23.0 | 2,517 |
| 13.0 | 557.0 | 22.9 | 2,486 |
| 12.0 | 529.3 | 22.6 | 2,392 |
| 11.0 | 504.6 | 22.3 | 2,305 |
| 10.0 | 480.6 | 22.2 | 2,214 |
| 9.0 | 454.6 | 22.0 | 2,108 |
| 8.0 | 424.2 | 22.0 | 1,976 |
| 7.0 | 386.9 | 21.9 | 1,806 |

## Target NRHO

All trajectories presented in this paper insert into a 9:2 lunar synodic resonant L2 southern NRHO, characterized by a perilune radius of approximately 3,233 km and a period of 6.6 days. This NRHO was selected based on favorable transfer characteristics as well as the ability to avoid lengthy eclipses by the Earth.[2] It exhibits nearly-stable behavior, and station-keeping algorithms enable long-term stays for either crewed or un-crewed assets.[3] This NRHO is considered a southern L2 halo orbit because its perilune is over the Moon's north pole and it spends most of its orbit above the Moon's south pole. This orbit is shown in Figure 1.

When necessary, an optimally phased 9:2 NRHO is constructed by targeting a partial state in a Moon-centered Earth-Moon rotating frame and varying the free components to achieve zero x- and z-velocity at the y-axis crossing after half of a period. The targeted velocity is zero in the x- and z-direction and free in the y-direction, where x is along the Earth-Moon line and z is parallel to the angular momentum vector of the system. The targeted position is free in the x-direction, zero in the y-direction, and 3,230 km in the z-direction. This strategy provides a straightforward way to generate a representative 9:2 NRHO at any required epoch in the ephemeris model, though the resultant NRHO is not necessarily stable for more than one period in the ephemeris model.

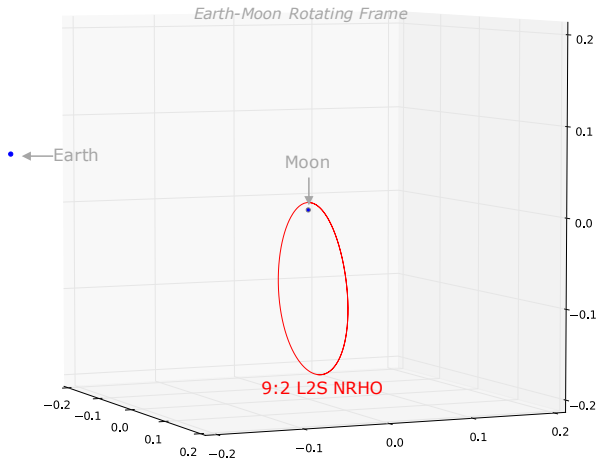


**Figure 1. A 9:2 Lunar Synodic Resonant L2 Southern NRHO in the Earth-Moon rotating frame.**

## SLS CO-MANIFESTED PAYLOAD TO NRHO INSERTION

The first option considered for inserting into the NRHO is to launch as an SLS co-manifested payload. This section describes a reference trajectory design and discusses the results of a launch date sensitivity analysis.

### Reference Trajectory

The reference trajectory begins when the spacecraft separates from the SLS upper stage (US). Prior to separation, it is assumed that the US completes a TLI burn to place itself and the spacecraft on a trajectory targeting an polar outbound LGA to achieve heliocentric disposal of the US with an Earth relative $C_3$ greater than zero. Twelve hours after separation, the spacecraft is allowed to apply a small impulsive reaction control system (RCS) burn of up to 10 m/s to retarget the LGA and avoid escaping heliocentrically with the US. This retargeting maneuver cannot be completed with SEP because of a required 14-day checkout period before the first SEP thrust arc. The trajectory design is further constrained by a requirement to insert into the NRHO within 100-day of US separation, thus eliminating the option of a long duration ballistic Earth to NRHO insertion.

The reference trajectory is designed and optimized using Copernicus,[7] a high-fidelity trajectory optimization tool, with a parallel monotonic basin hopping wrapper.[8] Point mass gravity is included for the Earth, Moon and Sun using the DE430 ephemeris model. The objective function is minimum propellant mass, which is determined as the sum of that required for both the RCS retargeting maneuver and any SEP thrusting.

For the reference trajectory, a launch date of August 10, 2021 was selected based on a notional Exploration Mission timeline. For this solution, the impulsive RCS retargeting maneuver optimizes to 3.96 m/s. At a mission elapsed time (MET) of approximately 5 days, the LGA places the spacecraft on a trajectory to eventually re-encounter the Moon. At 14 days MET, the first thrust arc of 15.2 days begins, followed by a 43.6 day coast before a 3.1 day NRHO insertion burn. This trajectory requires a total of 75.9 days, 106.9 kg of propellant (11.4 kg RCS and 95.5 kg xenon), and a total of 370 m/s $\Delta$V to deliver 6,393.1 kg to the NRHO. A plot of the trajectory is shown in Figure 2. A summary of the major events is shown in Table 3.

**Table 3. Event summary for the reference SLS NRHO insertion trajectory**

| Date | Event | MET (d) | $\Delta$t (d) | Mass (kg) | Prop. (kg) | $R_{Earth}$ (km) | $R_{Moon}$ (km) |
|---|---|---|---|---|---|---|---|
| 2021-08-10 | Separation | 0.0 | - | 6,500.0 | - | 15,135 | 365,040 |
| 2021-08-10 | Coast 1 | 0.0 | 14.0 | 6,500.0 | - | 15,135 | 365,040 |
| 2021-08-11 | RCS Burn | 0.5 | - | 6,500.0 | 11.4 | 134,746 | 317,667 |
| 2021-08-24 | Thrust 1 | 14.0 | 15.2 | 6,488.6 | 79.4 | 523,073 | 344,069 |
| 2021-09-08 | Coast 2 | 29.2 | 43.6 | 6,409.2 | - | 929,216 | 1,092,187 |
| 2021-10-22 | Thrust 2 | 72.8 | 3.1 | 6,409.1 | 16.0 | 417,928 | 75,891 |
| 2021-10-25 | Insertion | 75.9 | - | 6,393.1 | - | 406,931 | 17,396 |

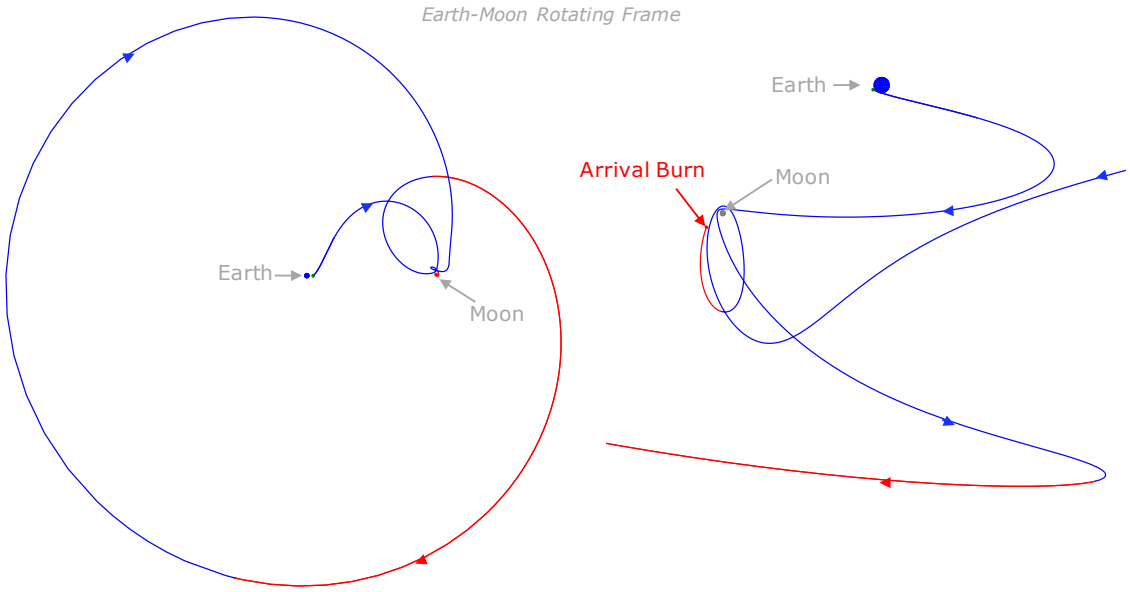


**Figure 2. Reference 75.9-day NRHO insertion trajectory in the Earth-Moon rotating frame. Coast and thrust arcs are colored in blue and red, respectively. An overview is shown on the left and a closeup near the Moon is shown on the right.**

### Reference Trajectory Launch Date Sensitivity

With the reference SLS co-manifested NRHO insertion designed, analysis was completed to understand how sensitive this trajectory type is to changes in launch date. It is important to understand these sensitivities because a co-manifested payload may not be able to dictate exact launch date or conditions. A representative US separation state was generated each day over a 6-month period and the insertion trajectory was re-opitmized for each. Solutions were generated sequentially and seeded with the that from the previous day to maintain consistency between the trajectory geometry and aid in convergence.

With a converged solution for each separation state, the minimized propellant mass (sum of RCS and xenon) can be plotted as a function of launch day as shown in Figure 3. This plot shows a cyclical pattern with propellant mass ranging from 87 - 152 kg, compared to the reference case of 106.9 kg. A relationship with the lunar synodic period is suggested by the 15-day period between minimum propellant points.

In an effort to better understand the cyclical pattern, Figure 4 shows 6-months worth of optimal trajectories plotted in the Earth-centered Sun-Earth rotating frame. Each solution separates from the launch vehicle near Earth at the center of the plot, completes an outbound LGA, reaches apogee nearly 180 degrees from the LGA, and falls back in towards the orbit of the Moon for NRHO insertion. Each solution is colored by the total propellant mass used, with minimum propellant in black and maximum propellant in white. Coloring the solutions with a gradient from black to white highlights the most efficient trajectories and hides the least efficient trajectories. In doing so, it becomes immediately clear that the most efficient trajectories are those with apogees in the upper left and lower right quadrants of the plot. The solutions fade to white in the upper right and lower left quadrants as they require increasing propellant mass.

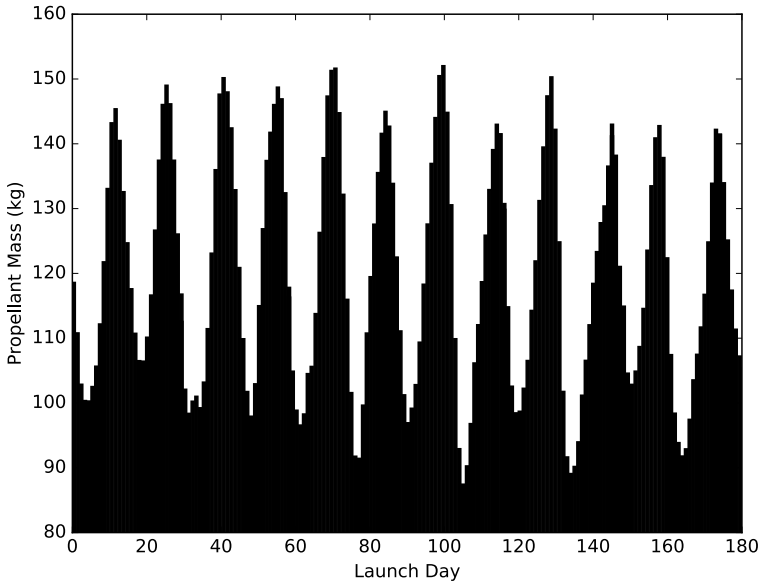


**Figure 3. Propellant mass used as a function of launch day for a 6-month launch window.**

To further quantify the observed pattern, the four quadrants in the Sun-Earth rotating frame can be numbered (I, II, III, IV) and a solar phase angle ($\Phi$) can be defined as an angle from the Sun-Earth line in the Sun-Earth rotating frame. The angle $\Phi$ ranges from $\pm 180^\circ$ and is negative in the counterclockwise direction, as shown on the right of Figure 5. With these values defined, a plot of the total propellant mass as a function of $\Phi$ at the apogee of the orbit following the LGA is plotted for each solution on the left of Figure 5. This plot shows that the minimum propellant solutions are achieved when $\Phi$ at apogee is near -110° or +70° in quadrants II and IV, respectively. The maximum propellant solutions are found when $\Phi$ at apogee is near -20° or +160° in quadrants I and III, respectively.

The quadrant dependency seen in Figure 4 and Figure 5 can be attributed to the effect of solar gravity. While the spacecraft is in quadrants II and IV, solar gravity tends to raise perigee. Solar gravity tends to lower perigee in quadrants I and III.[6,9,10] Advantageous use of this effect reduces the need to propulsively raise perigee to the radius of the Moon's orbit. For this trajectory geometry, achieving an apogee in a desired quadrant determines the quadrant in which the Moon is encountered, thus giving rise to a cyclical pattern with a period approximately equal to half of the 29.5 day lunar synodic period.

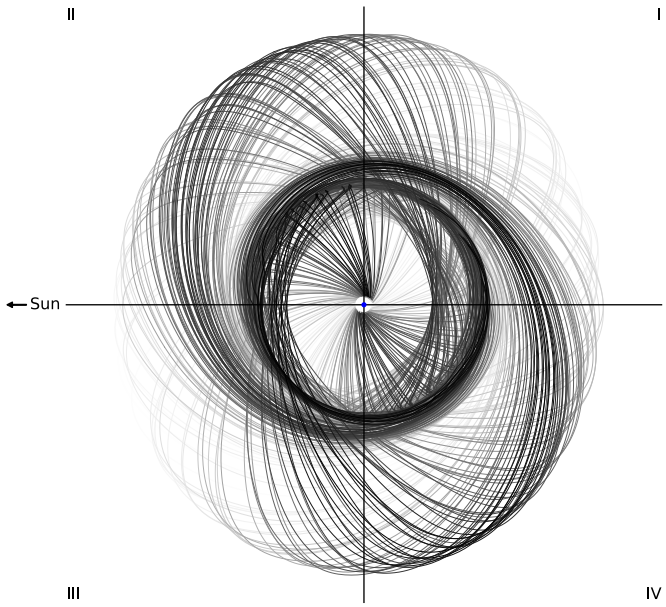


**Figure 4. 6-months of optimized insertion trajectories displayed in the Earth-centered Sun-Earth rotating frame. Each solution is colored by the total propellant mass used, with with a gradient from black to white, where minimum propellant is black and maximum propellant is white.**

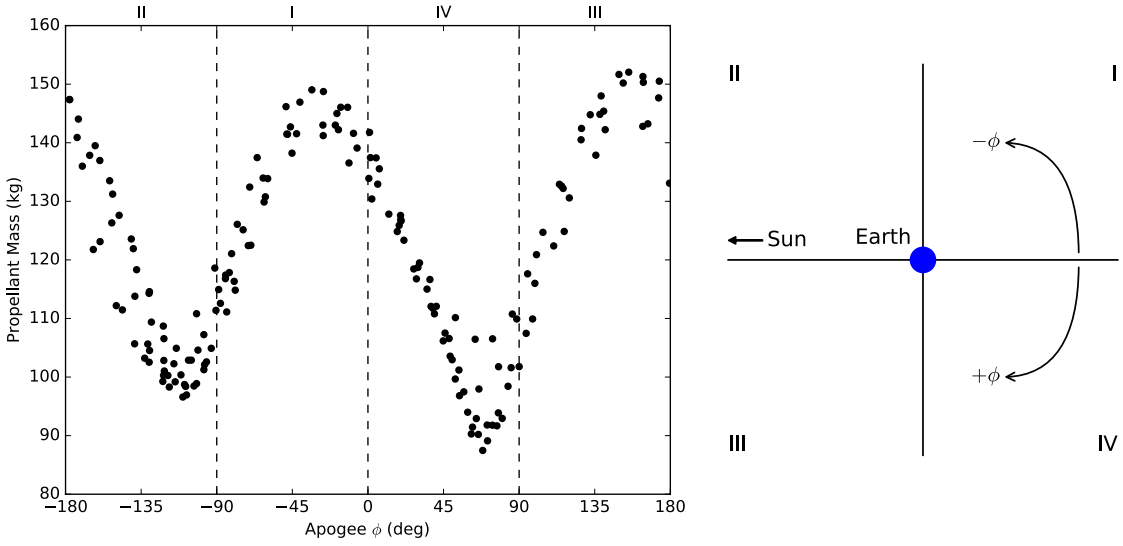


**Figure 5. Plot of the total propellant used a function of apogee solar phase angle, $\Phi$, the definition of which is shown on the right.**

## EARTH ELLIPTICAL ORBIT TO NRHO INSERTION

The second option considered is to launch into an Earth Elliptical Orbit (EEO) and use the SEP system to complete a spiral out trajectory leading to NRHO insertion. This section provides an overview of this insertion type, an explanation of the methodology used to design the trajectories, a generic set of solutions that are launch vehicle independent, and finally a set of trajectories that are designed for launch on a Falcon 9 and Atlas V 551. The results presented demonstrate the trades between TOF, NRHO mass, propellant required, $\Delta$V, and solar array degradation.

### Insertion Overview

This option for NRHO insertion is assumed to utilize a less powerful Commercial Launch Vehicle (CLV) to inject into an EEO with a perigee altitude of 400 km, which is the minimum perigee altitude allowed for SEP thrusting. The EEO apogee altitude ($H_a$) depends upon launch vehicle performance and required mass delivered to NRHO. The EEO inclination is approximately 28 degrees and the remaining orbital elements are considered optimization variables. After separation from the launch vehicle, a required 14-day checkout period is followed by a low thrust spiral trajectory that delivers the spacecraft to an Intermediate Target State (ITS) which arrives nearly ballistically to the NRHO 45.25 days later with a 2 m/s insertion burn.

Figure 6 shows an example EEO to NRHO trajectory in the Earth-centered J2000 inertial frame. Thrust and coast periods are shown in red and blue, respectively. The ITS is located at the transition from thrust to coast (red to blue) after the low thrust spiral.

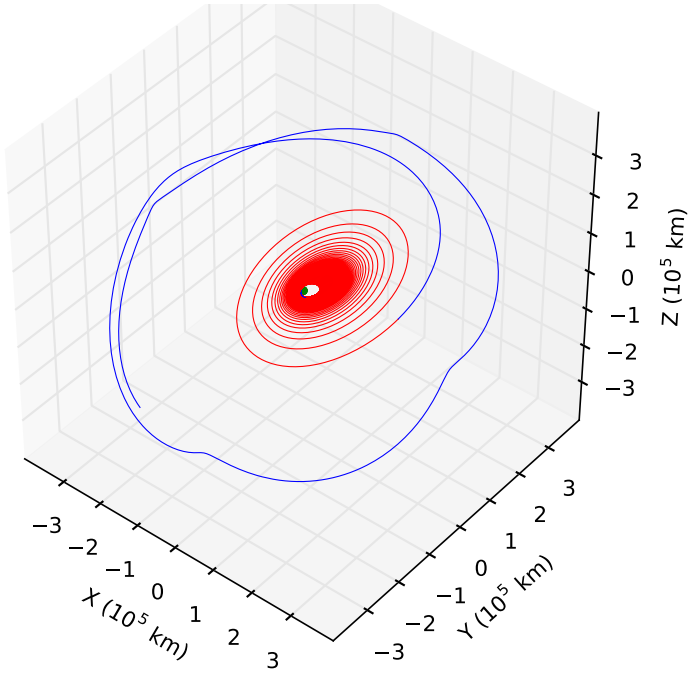


**Figure 6. An example EEO to NRHO insertion shown in the Earth-centered J2000 inertial frame. Thrust and coast periods are shown in red and blue, respectively.**

## Methodology

A specialized version of Optimal Trajectories by Implicit Simulation (OTIS[11]) was used to perform the EEO to NRHO analysis. This version of the program employs specialized features for improved SEP transfer modeling; e.g. optimized closed loop targeting, detailed solar array modeling (including degradation), optimized array pointing, and radiation modeling, all of which are used in this analysis. In addition to Earth's gravity, the influence of the Moon, Sun and Jupiter are also accounted for. There is no thrusting allowed while the spacecraft is in shadow. While OTIS can also insert optimal coasting periods to achieve more efficient propellant usage, this feature was not employed in this study since shorter transfer times are preferred. Exploring additional solution options may be the topic of future studies where transfer time is of secondary concern.

The ITS serves as the end point of a spiral trajectory that starts at an EEO, achieved by launching on a CLV. However, the spiral trajectory was actually modeled as starting from this ITS, with a defined spacecraft mass (referred to as "NRHO mass"), and propagated backwards to target an EEO via its semi-major axis, eccentricity, and inclination while minimizing SEP provided $\Delta$V. The resulting trajectory's time history may be reversed, as desired, to show the actual timeline for the mission. For purposes of this study, the EEO from which the spacecraft spiral trajectory begins, after the 14-day checkout, is assumed to be the same as the CLV delivery orbit. If a launch vehicle specific trajectory is desired, the EEO $H_a$ can be varied to ensure the required EEO delivered mass, consisting of the spacecraft's NRHO mass and the Xe required for the spiral, is on the CLV's performance curve (indicating zero excess CLV performance).

The use of the ITS allows for EEO to NRHO insertions to be designed over a range of NRHO masses while maintaining the same NRHO arrival geometry and epoch. The appropriate ITS, shown in Table 4, was determined with Copernicus[7] using a differential evolution solver. Starting from a long-duration NRHO ephemeris, a -0.25 day finite insertion burn was optimized in order to minimize the energy with respect to Earth and achieve an inclination of 28 degrees after a -45.0 day ballistic propagation. The propellant required for this insertion burn is small compared to that required for the spiral, so it is neglected for the purposes of this analysis. Therefore, the mass at the ITS (NRHO mass) is considered to be the mass delivered to NRHO and this portion of the trajectory will be referred to as "ballistic" from this point forward.

**Table 4. Intermediate target state in the Earth-centered J2000 frame.**

| | |
|---|---|
| Julian Date | 2.46065514394 E+06 |
| X (km) | 2.52499218023 E+05 |
| Y (km) | -1.67452406620 E+04 |
| Z (km) | 7.72249329231 E+04 |
| VX (km/s) | 2.16787408451 E-01 |
| VY (km/s) | 1.00494032789 E+00 |
| VZ (km/s) | 4.87964647320 E-01 |

In addition to optimizing the trajectory, the OTIS trajectory simulation has a detailed solar array subsystem model along with optimal array sun pointing capability. Table 5 lists some of the main solar array definition parameters such as cell type and area, blanket type, and cover slide thickness that were used as inputs to this model. Of specific interest is the solar array performance degradation; this is modeled via a set of degradation parameters to account for various sources of degradation. One of the main sources of array degradation is due to radiation, especially when traversing through the Van Allen belts. An AE8/AP8 radiation model[12] is used to account for solar array degradation

due to radiation. For this study, an End Of Life (EOL) power level of 41 kW was chosen with 40 kW to supply the EP system and an additional 1 kW for non-EP spacecraft use. The Beginning Of Life (BOL) power is determined as the power required at EEO departure to guarantee the necessary EOL power at NRHO insertion after all degradation sources are accounted for. The EP system, however, does not use of any of the excess power (above 40 kW) that may be available early in the mission.

**Table 5. Summary of the relevant solar array model assumptions (a subset of the full model inputs.)**

| Parameter | Value | Note |
|---|---|---|
| EOL Power | 41 kW | Power required after NRHO insertion |
| BOL Power | Calculated | Determined by spiral trajectory |
| Cell Type | XTJ | - |
| Array Area | 72 $cm^2$ | - |
| Blanket Type | ROSA | - |
| Cover Slide Thickness | 3 / 0 mils | Front / Back (back has natural equivalent shielding of 16.5 mils) |
| Operating Voltage | 120 V | - |

To better illustrate the capability of the solar array subsystem model, the plots in Figure 7 show example operating power profiles for an NRHO mass of 6,500 kg and an EEO $H_a$ range from 5,000 to 50,000 km. At each instance in the simulation, the solar array model internally generates a current (I) versus voltage (V) curve (I-V curve). For EP performance purposes, a 120V operating voltage is assumed with a corresponding operating current and operating power level. The shadowing impact has been removed for plotting clarity purposes only; all analyses included the shadowing impact on the EP system. The right plot in Figure 7 shows a zoomed in view of the operating power profiles to better display the higher EEO apogee cases. The power degradation from BOL to EOL is more pronounced for cases with lower EEO $H_a$. In these cases, more time is spent in the high radiation environment leading to increased degradation. Degradation decreases dramatically as EEO $H_a$ approaches 50,000 km. This trend would continue for even higher altitudes, which have been omitted for plotting clarity.

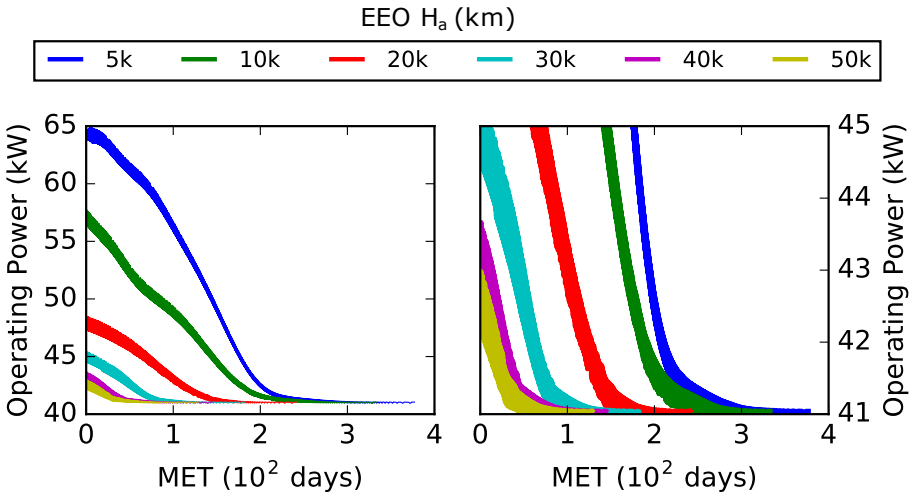


**Figure 7. Example plots of solar array Operating Power as a function of MET for a range of EEO $H_a$ from 5,000 to 50,000 km (5k - 50k). The plot on the right shows the same data as left, but zoomed in to show details for higher altitudes. All curves are shown for an NRHO mass of 6,500 kg and EOL Operating Power of 41 kW.**

### Launch Vehicle Independent Analysis

To assist in mission planning, a launch vehicle independent analysis was completed. For this purpose, EEO to NRHO insertion trajectories were generated over a grid of EEO $H_a$ and NRHO masses from 10,000 - 100,000 km and 5,000 - 10,000 kg, respectively, without targeting an EEO specific to any launch vehicle performance curve. This results in a generic set of data that can assist in determining the required launch vehicle performance subject to mission constraints such as maximum TOF, propellant mass, or solar array degradation.

Figure 8 shows contour plots of TOF (left) and required xenon propellant mass (right) as functions of EEO $H_a$ and NRHO mass based on trajectories in this data set. The TOF includes a 14 day checkout in EEO, the spiral time to ITS, and a 45.25 day ballistic NRHO insertion. The TOF contours can be used to determine, for example, the minimum EEO $H_a$ required to deliver 7,000 kg to NRHO in less than 180 days: approximately 70,000 km. Examining the xenon propellant mass contours at the same combination of EEO $H_a$ and NRHO mass shows that approximately 600 kg of propellant is required to complete the transfer. The propellant mass can be added to the NRHO mass (7,000 kg + 600 kg = 7,600 kg) to estimate the required launch vehicle performance to a 70,000 km $H_a$ EEO. The estimated spiral time from EEO to ITS for this case is approximately 120 days (i.e. 180 days total TOF - 14 days for checkout - 45.25 days for ballistic NRHO insertion).

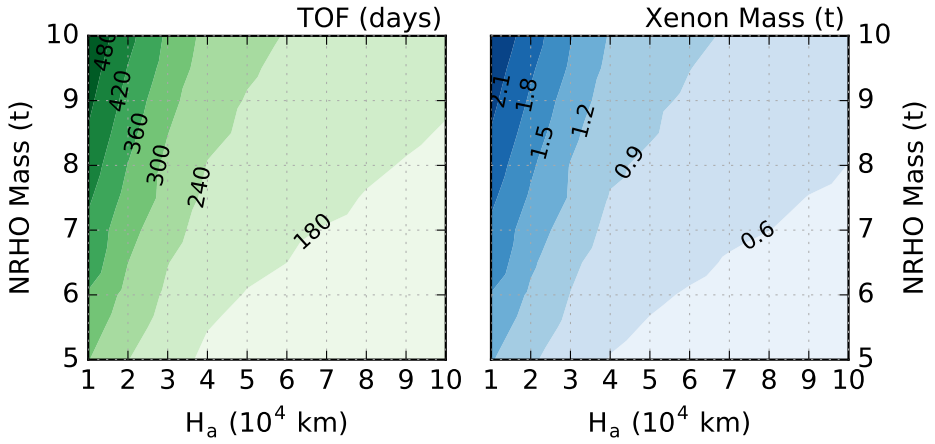


**Figure 8. Contour plots of TOF (left) and required xenon propellant mass (right) as functions of EEO $H_a$ and NRHO mass.**

Figure 9 shows plots of percent change in power ($\Delta$Power, left) and $\Delta$V (right) as functions of EEO $H_a$. The percent power degradation is computed based on the previously assumed EOL operating power of 41 kW. It is assumed that this behavior is independent of the actual size of the array, since a larger or smaller array would simply add or subtract strings of individual cells which are assumed to degrade at the same rate. The thick line on the $\Delta$Power plot encompasses all data points from this analysis, showing that, while the degradation is mostly dependent upon EEO $H_a$, there is still some dependence upon NRHO mass. This is because a more massive spacecraft must spend more time spiraling through lower altitudes; i.e. a less massive spacecraft will see less $\Delta$Power for a given EEO $H_a$.

The plot on the right in Figure 9 shows that the $\Delta$V required for a transfer is almost solely a function of EEO $H_a$. This plot can be used to estimate the required propellant mass and TOF for an

NRHO mass not included in the dataset or if a different SEP system is of interest. The TOF would be estimated by dividing the propellant mass by the mass flow rate of the desired SEP system and adding 14 days for checkout and 45.25 days from the ITS to the NRHO. With this TOF computation, however, the spiral time represents thruster-on only. Additional time must be added to account for time in eclipse when no thrusting is allowed.

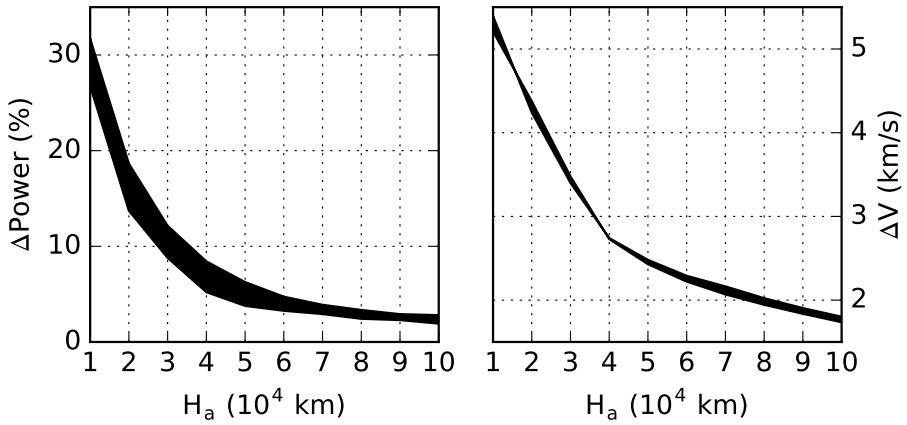


**Figure 9. Plots of percent change in power (left) and $\Delta$V (right) as functions of EEO $H_a$.**

To determine how much additional time must be added to account for time in eclipse when no thrusting is allowed, Table 6 shows an average of the percentage of spiral time the spacecraft spends in eclipse (shadow) based on some of the analyzed EEO cases. While, in general, eclipse time is a function of various parameters such as the SEP system, specific orbit choice, seasonal variation (date), etc., these eclipse percentages can be used to improve the quality of the estimate for EEO type orbits with a low perigee altitude (400km). For example, if the $\Delta$V was used to estimate the propellant mass and, along with the mass flow rate, a thruster-on time of 160 days was computed for a $H_a$ = 30,000 km, the total spiral time including eclipse would be 160 / (1 – 0.0205) = 165.9 days. Adding the SEP checkout and ITS to NRHO times results in a total TOF of 225 days. It should be stressed that these types of estimates are only valid for similar mission types beginning in an EEO with low perigee altitude.

**Table 6. Average percentage of the spiral trajectory time the spacecraft spends in eclipse (shadow) based on some of the analyzed EEO cases for varying EEO $H_a$.**

| $H_a$ ($10^4$ km) | 1 | 2 | 3 | 4 | 5 | 6 | 7 | 8 | 9 | 10 |
|---|---|---|---|---|---|---|---|---|---|---|
| Eclipse % | 6.18 | 3.55 | 2.05 | 0.97 | 0.56 | 0.41 | 0.28 | 0.17 | 0.11 | 0.10 |

### Launch on Falcon 9 or Atlas V 551

In addition to the launch vehicle independent analysis discussed the previous section, analysis was completed for two specific CLVs, Falcon 9 (F9) and Atlas V 551 (AV). For this analysis, the spacecraft trajectories from EEO to NRHO were analyzed for a range of EEO $H_a$ from 10,000 to 100,000 km. Of primary interest are those cases where the required spacecraft wet mass in EEO matches the CLV performance for the same EEO. For these cases, the CLV delivers just enough mass

to cover the desired NRHO spacecraft mass plus the required Xe propellant for the SEP transfer from EEO to NRHO. The $H_a$ at which the masses match is the upper limit on $H_a$ for the selected NRHO mass. Above this $H_a$, the CLV cannot deliver enough mass to make the mission possible. Below this this $H_a$, there will be excess CLV performance for the selected NRHO mass.

The two specific launch vehicles selected for this analysis, F9 and AV, were chosen to represent the lower and higher end of CLV capability that would be required for injection into elliptical orbits. The mass delivered, from publicly available performance curves, to elliptical orbits with a 185 km perigee altitude was decreased by 200 kg and 250 kg for AV and F9, respectively (based on a separate launch vehicle analysis), to estimate performance to a perigee altitude of 400 km (see Table 7). The F9 and AV are assumed to launch to an inclination of 27 and 28.5 degrees, respectively. For each launch vehicle, EEO to NRHO insertions were generated across their performance curves in order to understand the trades between TOF, $\Delta$V, xenon propellant mass, and mass delivered to the NRHO. In addition, the detailed solar array model was used to estimate the operational array power required at launch in order to guarantee that 41 kW is available at NRHO for each trajectory; 40 kW to the EP system and 1 kW for spacecraft use. The results of these trades are detailed in this section.

**Table 7. Mass delivered by F9 and AV to elliptical orbits with 400 km perigee altitude and apogee altitude ($H_a$).**

| $H_a$ (km) | AV (kg) | F9 (kg) |
|---|---|---|
| 100,000 | 6,935 | 3,880 |
| 90,000 | 7,030 | 3,980 |
| 80,000 | 7,150 | 4,100 |
| 70,000 | 7,290 | 4,255 |
| 60,000 | 7,475 | 4,455 |
| 50,000 | 7,740 | 4,715 |
| 40,000 | 8,120 | 5,040 |
| 30,000 | 8,695 | 5,620 |
| 20,000 | 9,705 | 6,585 |
| 10,000 | 11,955 | 8,550 |
| 5,000 | 14,510 | - |

*Mass and Time Sensitivity:* Figure 10 shows plots of NRHO mass as a function of TOF (top left), required xenon propellant mass (top right), EEO $H_a$ (bottom left), and SEP $\Delta$V (bottom right, assuming an $I_{sp}$ of 2507 s). NRHO masses less than 5,000 kg are not of interest to this study as they are expected to be less than the dry mass of a representative spacecraft. NRHO masses were increased for each CLV until EEO $H_a$ approached the lower end of CLV performance data. Because all plots include the same NRHO mass data points and the same scale, they can be used in combination to gain insight into the trades between the plotted quantities. For example, it's clear that the maximum NRHO mass requires the longest TOF. Consequently, the longer TOF for this case corresponds to the maximum propellant mass and $\Delta$V.

The maximum NRHO mass was found to be 9,500 kg and 6,500 kg, requiring 500 days and 375 days, for the AV and F9, respectively. These times include the 14 day checkout in EEO, spiral time to ITS and the 45.25 day ballistic NRHO insertion. At the maximum NRHO mass, the xenon mass required for insertion is 2,225 kg and 1,600 kg, both applying a $\Delta$V of 5.2 km/s, for the AV and F9, respectively. If a TOF of less than 1-year is desired, NRHO masses of approximately 8,100 kg (AV) and 6,200 kg (F9) are possible. If only 1,000 kg of xenon propellant can be used, NRHO masses of approximately 7,200 kg (AV) and 5,500 kg (F9) are possible.

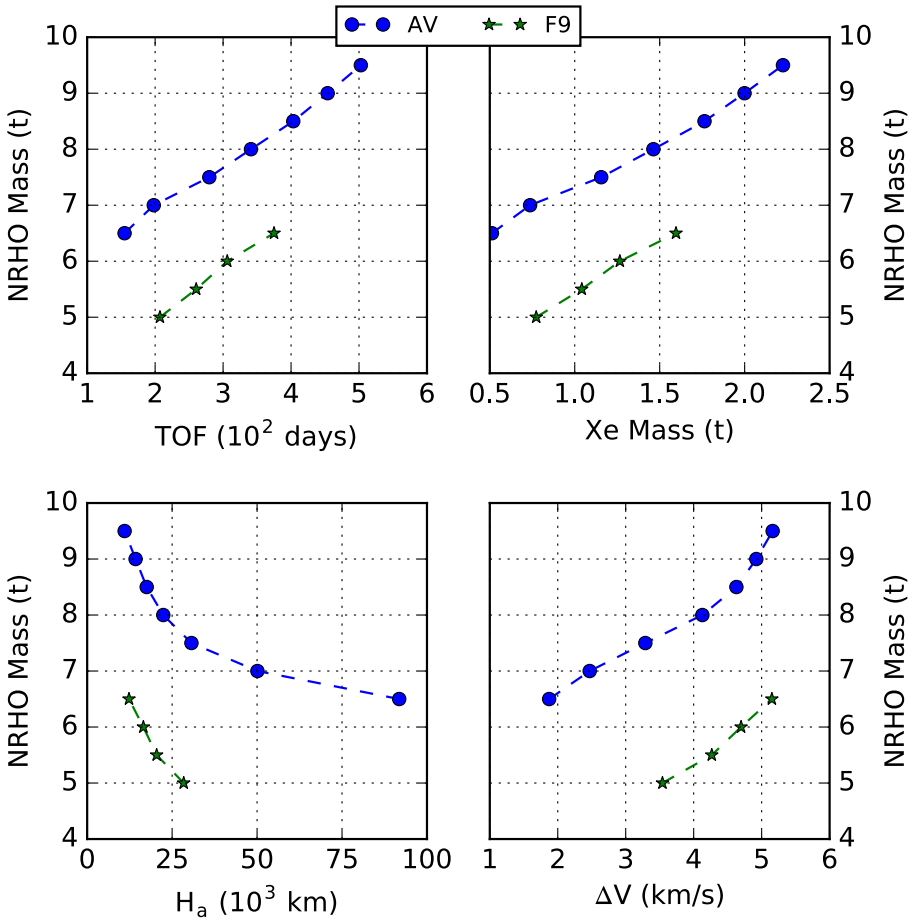


**Figure 10. Plots of mass delivered to NRHO (NRHO Mass) as a function of TOF (top left), Xenon Mass (top right), EEO $H_a$ (bottom left), and SEP $\Delta V$ (bottom right).**

*Power Sensitivity:* While the time histories of the operating power are useful to know, for purposes of this study, the behavior of the BOL operating power is of greater interest for mission planning purposes. The left plot in Figure 11 shows the BOL operating power as a function of EEO $H_a$ for the same AV and F9 cases shown previously in Figure 10. This plot is useful to determine the range of acceptable EEO $H_a$ based on BOL power limitations. As expected, BOL operating power increases and EEO $H_a$ decreases. It is interesting to note that the BOL operating power is more dependent upon the EEO apogee than the chosen CLV. The right plot in Figure 11 shows the BOL operating power as a function of NRHO mass. This plot demonstrates that greater NRHO masses require larger BOL operating power because they must launch to lower a EEO $H_a$. In addition, examination of the overlapping points between F9 and AV at NRHO mass of 6.5 t shows that a F9 launch would require a BOL operating power that is 14 kW greater than an AV launch for the same NRHO mass because it must launch to a lower altitude.

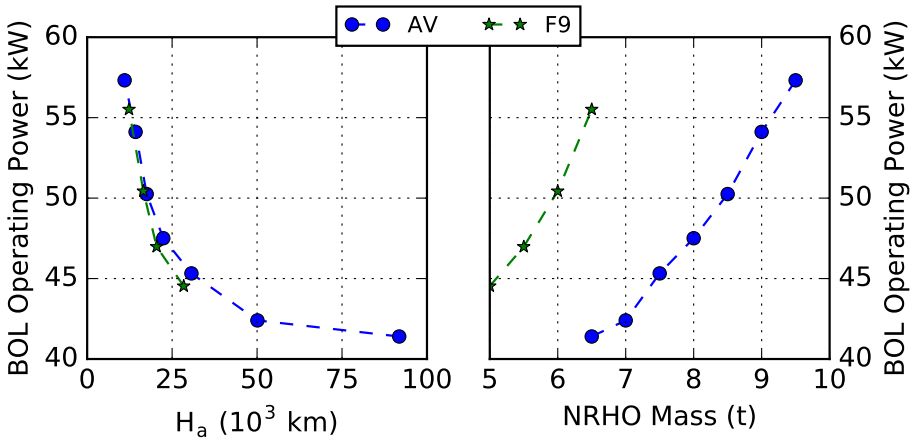


**Figure 11. Plots of required BOL Operating Power as a function of EEO $H_a$ (left) and NRHO Mass (right). The BOL Operating Power is that which is required to achieve 41 kW EOL**

*Mission Planning Considerations:* The results presented above show that both the AV and F9 offer enough performance to enable an EEO to NRHO insertion over a range of NRHO masses. The AV is more capable than the F9 resulting in a larger feasible region; i.e. a wider range of possible EEO $H_a$. This in turn enables more options in terms of TOF and BOL operating power requirements. A general guideline is to take full advantage of the CLV performance to reduce the burden on the SEP system as well as the the solar array degradation. Stated differently, the more work the CLV does, the less propellant required to deliver a given spacecraft mass to NRHO, and the lower the BOL operating power. Also, the lower the BOL power requirement, the smaller, less massive and less costly the required solar arrays will be. For example, with an assumed solar array power density of 10 kg/kW, launching to an 11,000 km EEO could add up to an additional 160 kg of dry mass to the spacecraft compared to a higher feasible launch.

Another design parameter is the NRHO mass. A range of spacecraft NRHO masses from 5,000 to 9,500 kg were considered. Within this range, the feasible points using all F9 performance ranged from EEO $H_a$ of 28,400 km (5,000 kg NRHO mass) down to 12,300 km (6,500 kg NRHO mass). For the AV, the range of EEO $H_a$ is 91,800 km (6,500 kg NRHO mass) down to 11,000 km (9,500 kg NRHO mass). Altitudes below these values are also feasible and allow for excess CLV performance at the cost of additional propellant and TOF.

## CONCLUSION

Two options for low thrust orbit insertion into an NRHO have been presented. The first option launches as co-manifested payload on SLS, while the second option is to launch on a CLV to an EEO and use a SEP spiral to the NRHO.

For the first option, launching as a co-manifested SLS payload, a spacecraft with a 6,500 kg wet mass can be inserted into NRHO with as little as 90 kg of propellant in 76 days. There is, however, a dependence upon the solar phase angle that can lead to required propellant mass to nearly double if launched at the least optimal time. The oscillation in propellant mass has a period of half of the lunar synodic period, which leads to the most optimal launch times occurring approximately twice

per month. Though these insertion trajectories were designed with SLS-specific constraints, similar trends are expected to be observed for any similar high energy launch, with or without an outbound lunar gravity assist, to insert into NRHO.

For the second option, a launch vehicle independent analysis for a range of EEO $H_a$ and NRHO masses was presented. These results can be used to estimate the EEO to NRHO insertion characteristics over a range of NRHO masses. In addition, this information can help to determine the necessary launch vehicle performance given constraints on TOF, xenon propellant mass, and solar array degradation. It was shown that the choice of EEO $H_a$ determines the bulk of the insertion characteristics. In addition, it was found that launching to a low EEO $H_a$ can result in significant solar array degradation of as much as 30% over the duration of the insertion.

In addition, for the second option, analysis was completed specifically for two CLVs, the AV and F9. Both CLVs have feasible regions that can to deliver enough mass to make the EEO to NRHO transfer possible using SEP. The AV has a wider range of mission planning choices due to its higher performance. However, the trades between mission constraints such as NRHO mass, TOF, $\Delta$V, and BOL operating power must be considered when choosing the most appropriate insertion trajectory and CLV. It was found that the AV can enable a maximum NRHO mass of 9,500 kg in 500 days TOF, and the F9 can enable a maximum NRHO mass of 6,500 kg in approximately 380 days TOF. If a total TOF of less than 1-year is desired, the maximum NRHO mass is 8,100 kg and 6,200 kg for the AV and F9, respectively. If only 1,000 kg of propellant can be used, NRHO masses of approximately 7,200 kg (AV) and 5,500 kg (F9) are possible.

## ACKNOWLEDGEMENT

The authors thank Diane C. Davis from a.i. solutions for suggesting an explanation for the SLS insertion behavior, Thomas W. Kerslake from NASA Glenn Research Center for solar array information, and Eric Haddox, Zachary May, and Jarmaine Ollivierre from NASA Kennedy Space Center for launch vehicle performance information.

## REFERENCES

[1] D. J. Grebow, M. T. Ozimek, K. C. Howell, and D. C. Folta, "Multi-Body Orbit Architectures for Lunar South Pole Coverage," *16th AAS/AIAA Space Flight Mechanics Conference*, January 2006.

[2] R. Whitley and R. Martinez, "Options for Staging Orbits in Cis-Lunar Space," *37th IEEE Annual Aerospace Conference*, March 2016.

[3] J. Williams, D. E. Lee, R. J. Whitley, K. A. Bokelmann, D. C. Davis, and C. F. Berry, "Targeting Cislunar Near Rectilinear Halo Orbits for Human Space Exploration," *27th AAS/AIAA Space Flight Mechanics Meeting*, February 2017.

[4] M. L. McGuire, N. J. Strange, L. M. Burke, S. L. McCarty, G. B. Lantoine, M. Qu, H. Shen, D. A. Smith, and M. A. Vavrina, "Overview of the Mission Design Reference Trajectory for NASA's Asteroid Redirect Robotic Mission," *AAS/AIAA Astrodynamics Specialist Conference*, August 2017.

[5] M. L. McGuire, L. M. Burke, S. L. McCarty, K. J. Hack, R. J. Whitley, D. C. Davis, and C. Ocampo, "Low Thrust Cis-Lunar Transfers Using a 40 kW-Class Solar Electric Propulsion Spacecraft," *AAS/AIAA Astrodynamics Specialist Conference*, August 2017.

[6] J. S. Parker and R. L. Anderson, *Low-Energy Lunar Trajectory Design*. Hoboken, New Jersey: John Wiley and Sons, Inc., June 2014.

[7] C. Ocampo and J. Senent, "The Design and Development of COPERNICUS: A Comprehensive Trajectory Design and Optimization System," *57th International Astronautical Congress*, October 2006.

[8] S. L. McCarty and M. L. McGuire, "Parallel Monotonic Basin Hopping for Low Thrust Trajectory Optimization," *28th AIAA/AAS Space Flight Mechanics Meeting*, January 2018.

[9] D. C. Davis and K. C. Howell, "Trajectory evolution in the multi-body problem with applications in the Saturnian system," *Acta Astronautica*, Vol. 69, Issue 11-12, December 2011, pp. 1038–1049.

[10] D. C. Davis, C. Patterson, and K. Howell, "Solar Gravity Perturbations to Facilitate Long-Term Orbits: Application to Cassini," *AAS/AIAA Astrodynamics Specialist Conference*, August 2007.

[11] J. Riehl, S. Paris, and W. Sjauw, "Comparison of Implicit Integration Methods for Solving Aerospace Trajectory Optimization Problems," *AIAA/AAS Astrodynamics Specialist Conference and Exhibit*, August 2006.

[12] D. Bilitza, "Models of Trapped Particle Fluxes AE-8 (electrons) and AP-8 (protons) in Inner and Outer Radiation Belts," *National Space Science Data Center, Data set PT-11B*, March 1996.